

# Energy scales and quasiparticle properties in an extended Hubbard model for HTC

R. Citro<sup>a</sup> and M. Marinaro

Dipartimento di Fisica “E.R. Caianiello” and Unità INFN di Salerno Università di Salerno, Via S. Allende, 84081 Baronissi (Sa), Italy

Received 31 July 2003 / Received in final form 17 November 2003

Published online 19 February 2004 – © EDP Sciences, Società Italiana di Fisica, Springer-Verlag 2004

**Abstract.** By means of a strong-coupling approach, developed in previous works, we study the quasiparticle properties in an extended Hubbard model in presence of critical charge fluctuations near a stripe-quantum critical-point. We show that the quasiparticle dispersion has a kink along the diagonal Brillouin zone at the energy of the order 50 meV, for realistic values of the parameters. The energy and momentum distribution curves (EDC, MDC) along the diagonal are also analyzed. The results for the EDC derived quasiparticle width reveals an anomalous drop in the low-energy scattering rate at the same energy of the kink. This drop corresponds to a new energy scale in the system that reflects the interaction between the quasiparticles and the critical charge fluctuations. The results offer a possible interpretation of the ARPES and photoemission experiments on Bi2212.

**PACS.** 71.10.Fd Lattice fermion models (Hubbard model, etc.) – 71.10.Hf Non-Fermi-liquid ground states, electron phase diagrams and phase transitions in model systems

The knowledge of multiple energy scales in physical systems provides significant insight into the processes that govern their low-energy properties. Concerning high-temperature superconductors, whose unusual properties are continuously under debate, the possibility to have multiple energy scales has been well investigated in the superconducting state of Bi2212 throughout the Brillouin zone. Remarkably, the presence of a second energy scale has been revealed in ARPES experiments on the diagonal zone where the superconducting gap vanishes [2,3], with significant changes both in the spectral lineshape and the quasiparticle dispersion. Specifically, below  $T_c$  a kink in the dispersion of quasiparticle develops along the diagonal line at finite energy ( $\simeq 50 \pm 10$  meV) resulting in a change of the quasiparticle velocity up to a factor of two or more. This effect is enhanced in the underdoped sample and persists above  $T_c$  where the kink becomes rather broad. The electronic structure calculation [1] predicts a linear dispersion in this range, but experimental doping, temperature and  $\mathbf{k}$ -dependence of the kink dispersion put constraints on a microscopic theory. Various interpretations on the origin of the kink have been proposed. A possible interpretation is based on the electron-phonon interaction [4]. A second interpretation is based on the coupling of the electrons to a magnetic resonance [5–7] and the third one is simply related to the opening of the superconducting

gap which is of the order of the kink energy. In this note we present a possible interpretation of the experimental data based on the stripe-scenario in which an incommensurate charge density wave (ICDW) is proposed as the source of the quasiparticle scattering that gives origin to the kink [8]. Within this scenario, we analyze the quasiparticle properties in an extended Hubbard model in two dimensions in presence of an ICDW. We report the results of the MDC (Momentum Distribution Curves) and of the EDC (Electron Distribution Curves) and discuss the influence of the stripe order on the evolution of the quasiparticle peak, dispersion and width. Our results give evidence of a kink in the quasiparticle dispersion along the diagonal Brillouin zone when charge stripes start to be formed. The analysis is based on our recent work where the study of a charge vertex, as a function of the doping and momentum, has shown a singular behavior responsible for a stripe phase formation [9]. The occurrence of such instability can be theoretically understood as an interplay between phase separation (PS) and long-range Coulomb interaction at finite doping [10]. Recently, various experimental evidences for the existence of such instability in the phase diagram of high- $T_c$  cuprates have been obtained by STM [12] and other experimental techniques (see Ref. [11]). Our results are not affected by the superconducting gap that is zero along the diagonal. A direct comparison with experimental results on Bi2212 is discussed.

---

<sup>a</sup> e-mail: citro@sa.infn.it

We consider the two-dimensional single-band Hubbard model, generalized with the inclusion of a long-range Coulomb interaction, whose Hamiltonian is:

$$H = \sum_{\langle i,j \rangle', \sigma} t_{ij} c_{i\sigma}^\dagger c_{j\sigma} - \mu \sum_{\sigma} n_{i\sigma} + U \sum_i n_{i\uparrow} n_{i\downarrow} + \sum_{i,j} V_{i,j} n_i n_j, \quad (1)$$

where  $c_{i\sigma}^\dagger$  ( $c_{i\sigma}$ ) is an electron creation (annihilation) operator with spin  $\sigma$  at site  $i$ ,  $t_{ij}$  is the hopping up to next-to-nearest included,  $\mu$  is the chemical potential,  $U$  and  $V_{i,j}$  are the local and the long-range Coulomb interaction, respectively.

The model is treated within a strong-coupling perturbative approach based on a cumulant expansion (CE) [13,14]. This expansion leads to the following exact expression of the Matsubara one-particle Green's function  $G(\mathbf{k}, i\omega_n)$ :

$$G(\mathbf{k}, i\omega_n) = \frac{[G^0(i\omega_n) + Z(\mathbf{k}, i\omega_n)]}{1 - t_{\mathbf{k}}[G^0(i\omega_n) + Z(\mathbf{k}, i\omega_n)]}, \quad (2)$$

where  $G_\sigma^{(0)}(i\omega_n)$  is the local-Hubbard Green's function, the function  $Z(\mathbf{k}, i\omega_n)$  contains all the irreducible graphs with two roots, except  $G^0(i\omega_n)$ , which cannot be broken into two parts by cutting a single line hopping,  $t_{\mathbf{k}}$  is the Fourier transform of the hopping.

The physical quantities in which we are interested are the single particle spectral function and the imaginary part of the self-energy, the last one being related to the quasiparticle lifetime. The first one is obtained from equation (2) by taking the analytic continuation ( $i\omega_n \rightarrow \omega + i\eta$ ):

$$\begin{aligned} A(\mathbf{k}, \tilde{\omega}) &= -\frac{1}{\pi} \text{Im}G(\mathbf{k}, \tilde{\omega}) \\ &= -\frac{1}{\pi} \frac{\text{Im}Z(\mathbf{k}, \tilde{\omega})}{[1 - t_{\mathbf{k}}(G^0(\tilde{\omega}) + \text{Re}Z(\mathbf{k}, \tilde{\omega}))]^2 + (t_{\mathbf{k}} \text{Im}(\mathbf{k}, \tilde{\omega}))^2}, \end{aligned} \quad (3)$$

where  $\mathbf{k}$  is the in plane momentum and  $\omega = \tilde{\omega} + \mu$ ,  $\mu$  being the chemical potential.

The crucial problem in the CE approach is the determination of the function  $Z(\mathbf{k}, \omega)$ . Being interested in the effect of charge fluctuations, we consider the approximate expression of  $Z(\mathbf{k}, \omega)$ :

$$Z(\mathbf{k}, i\omega_n) = \beta^{-1} \sum_{\omega_{n'}, \mathbf{k}'} \Gamma(\mathbf{k}', i\omega_{n'}) G^{(1)}(\mathbf{k}' - \mathbf{k}, i\omega_{n'} - i\omega_n) t_{\mathbf{k}' - \mathbf{k}}^2. \quad (4)$$

where  $\Gamma(\mathbf{k}, \omega)$  is the charge vertex function in the particle-hole channel (whose expression is reported Ref. [19]) and  $G^{(1)}(k)$  is the one-particle Green's function obtained in the lowest order cumulant expansion [15], describing two Hubbard subbands separated by a charge transfer gap. In conventional Fermi liquid theory, the charge vertex  $\Gamma$  is

a regular function that behaves as  $\text{Im}Z \propto \tilde{\omega}^2 + (\pi T)^2$  for small  $\tilde{\omega}$  and  $T$ . However, when the vertex function becomes singular, a strong  $\mathbf{k}$  and/or  $\omega$  dependence gives rise to anomalous features in the single-particle properties, as we shall show below. In our previous work, the charge vertex function  $\Gamma(\mathbf{k}, i\omega_n)$  has been evaluated within a generalized random phase approximation (RPA) [9] and we have shown that its low-energy behavior is given by:

$$\Gamma(\mathbf{k}', \omega' \rightarrow 0) \simeq -\frac{1}{\Omega(\mathbf{k}') - i\gamma_{\mathbf{k}'}\omega'}, \quad (5)$$

where  $\Omega(\mathbf{k}) \simeq M(\delta) + \alpha(\mathbf{k} - \mathbf{q}_{\mathbf{c}})^2$ ,  $\gamma_{\mathbf{k}}$  is the inverse relaxation time of charge fluctuations. This form of the vertex function is similar to that obtained in an effective model for tight-binding electrons coupled to charge and spin fluctuations in reference [16]. At  $\omega' = 0$ , the vertex becomes singular at  $\delta = \delta_c$ , at the critical vector  $\mathbf{k}' = \mathbf{q}_{\mathbf{c}}$  corresponding to an instability towards ICDW. In particular, we have found  $M(\delta) \propto (\delta - \delta_c)$ , showing that the doping determines the distance from the criticality and introduces an energy scale in the system. For the values of the Hamiltonian parameters in the range of physical interest ( $U/t = 5 \div 8$ ,  $V/t = 1. \div 3.$ ) we have obtained values of pairs  $(\mathbf{q}_{\mathbf{c}}, \delta_c)$  consistent with the experiments in Bi2212 near the optimal doping (i.e.  $\delta_c = 0.12 \div 0.15$  and  $\mathbf{q}_{\mathbf{c}} = (\pi/4, \pm\pi/4) \div (\pi/2, \pm\pi/2)$ ). The components of the critical vector  $\mathbf{q}_{\mathbf{c}}$  determine the direction of the charge stripes, while the inverse of its modulus the distance between them.

In order to investigate the influence of the critical charge fluctuations on the spectral function, we have computed the imaginary part of  $Z(\mathbf{k}, \tilde{\omega})$  using the low-energy expression of the vertex function (5). The expression for  $\text{Im}Z(\mathbf{k}, \tilde{\omega})$  and that for the real part, obtained by the Kramers-Kronig relation, permit us to calculate the spectral function (3) and the imaginary part of the self-energy:

$$\text{Im}\Sigma(\mathbf{k}, \omega) = -\text{Im}[Z(\mathbf{k}, \omega) + G^0(\omega)]^{-1}. \quad (6)$$

From the last relation, keeping in mind the on-shell equality that follows from (3)

$$G^0(\omega(\mathbf{k})) + \text{Re}Z(\mathbf{k}, \omega(\mathbf{k})) = \frac{1}{t_{\mathbf{k}}}, \quad (7)$$

we obtain the on-shell inverse quasiparticle lifetime:

$$\frac{1}{\tau} = \text{Im}\Sigma(\mathbf{k}, \omega(\mathbf{k})) \simeq t_{\mathbf{k}}^2 \text{Im}Z(\mathbf{k}, \omega(\mathbf{k})), \quad (8)$$

with  $t_{\mathbf{k}}^2 \text{Im}Z(\mathbf{k}, \omega(\mathbf{k})) \ll 1$ .

Now, we use the general formulas obtained above to discuss the behavior of the single-particle spectral function near the Fermi surface in presence of critical charge fluctuations. First, we determine the chemical potential corresponding to a fixed value of the doping ( $\delta = (1-n) = 0.12$ ) by using the one-particle Green function  $G^{(1)}$ , and to reproduce the band structure of Bi2212 around optimal doping we take  $t' = -0.25t$ . For a given set of parameters, the correction  $\delta\mu$  to the chemical potential from the charge

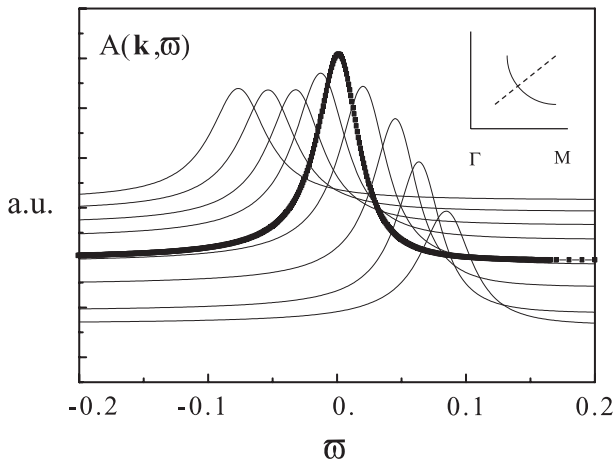


**Fig. 1.** Energy distribution curves (EDC) in arbitrary units (a.u.) at different values of  $\mathbf{k}$  around  $\mathbf{k}_F$ . The black dark curve corresponds to  $\mathbf{k} = \mathbf{k}_F = (1.66, 1.66)$ , the other curves correspond to the values 1.2, 1.3, 1.4, 1.5, 1.7, 1.8, 1.9, 2.0 of  $\mathbf{k}$  along the diagonal. The lattice constant is taken  $a = 1$ . The inset shows the Fermi surface cut along the diagonal line in the first Brillouin zone.

fluctuations is very small, as it will appear in the following. The other values of the Hamiltonian parameters (expressed in units of  $t$ ) are taken,  $T/t = 0.01$ ,  $U/t = 5$ . and  $V/t = 3$ . Finally, we take the critical vector  $\mathbf{q}_c$  near  $(\pi/2, \pm\pi/2)$  along the diagonal Brillouin zone. This choice is made in agreement with the results from angle-scanning-photoemission on Bi2212 [17] that reveals a modulation of the charge density wave with a wave-vector along the diagonal at optimal doping. The general results for the single-particle spectral function are characterized by the presence of a coherent peak associated with the quasiparticle near the Fermi surface and an incoherent peak, or hump, at higher energies. This second peak corresponds to a shadow band associated with  $\mathbf{q}_c$  (for details see also Ref. [16]). In the following we focus on the quasiparticle peak only.

In Figure 1, we plot the quasiparticle peak as a function of  $\tilde{\omega}$  for some values of  $\mathbf{k}$  around  $\mathbf{k}_F$  along the diagonal (energy distribution curves or EDCs), and in Figure 2 the quasiparticle peak is plotted as function of  $\mathbf{k}$  along the diagonal for  $\tilde{\omega} = 0$  (momentum distribution curves or MDCs). Figure 1 shows that the quasiparticle peak moves from left to right towards the Fermi energy, losing spectral weight as it crosses the Fermi level. The loss of spectral weight along this direction is due to the transfer of spectral weight to the shadow peak. We also note that the EDC curves at fixed values of  $\mathbf{k}$  have an asymmetric Lorentzian lineshape reflecting the non-trivial  $\omega$  dependence of the self-energy. This behavior of the EDC and MDC curves is in qualitative agreement with ARPES data on Bi2212 in references [2,3].

To get further information on the quasiparticle, in Figures 3-4 we plot the quasiparticle spectrum given by the equation:

$$[1 - t_{\mathbf{k}}(G^0(\tilde{\omega}) + \text{Re}Z(\mathbf{k}, \tilde{\omega}))] = 0, \quad (9)$$

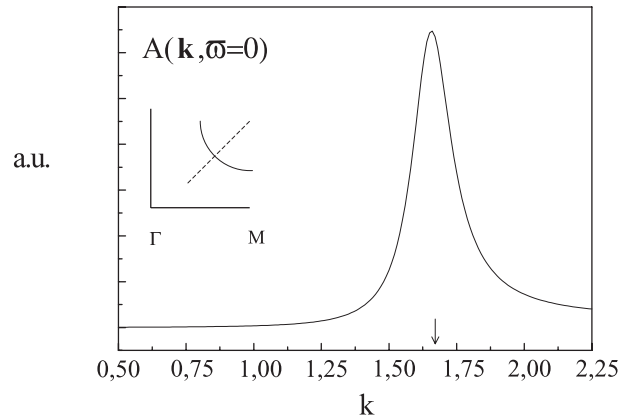


**Fig. 2.** Momentum distribution curve (MDC) in arbitrary units (a.u.) for  $\tilde{\omega} = 0$  and varying  $\mathbf{k}$  around  $k_F$  along the diagonal. The arrow represents the  $k_F$  position.

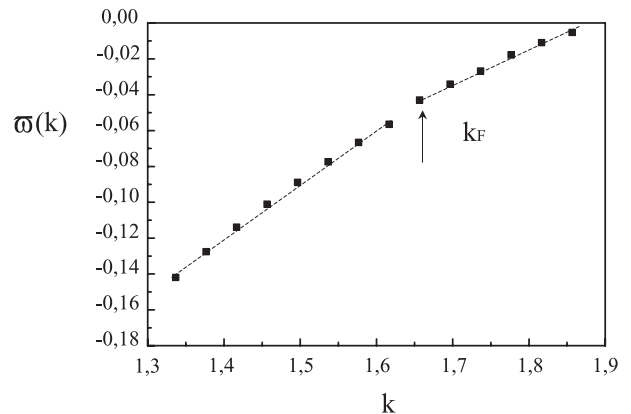


**Fig. 3.** Quasiparticle dispersion along the nodal Brillouin zone. The dashed line represents the linear fit of the high and low energy parts of the dispersion and the arrow the position of the Fermi momentum.

By looking into Figure 3, we clearly see a feature in the quasiparticle spectrum dispersing towards the Fermi energy with a break in the slope near  $-0.05$  eV. This break is known as a *kink* in the quasiparticle dispersion, indicating a change in the velocity. This behavior is clearly different from what one would expect from any electronic structure calculation. For  $\mathbf{k}$  near  $k_F$  and varying normal to the Fermi surface, one would expect the simple linear behavior  $\epsilon(\mathbf{k}) = v_F(k - k_F)$  to hold. Similar kinks in the quasiparticle dispersions have been seen by ARPES experiments in the normal metals and are attributed to the electron-phonon interaction [18]. An interpretation of data in Bi2212 in terms of the coupling of electrons to phonons has also been given in reference [4]. In our model we give a natural interpretation of the quasiparticle kink in terms of the scattering of the electrons with a charge collective mode described by the vertex  $\Gamma(\mathbf{k}, \omega)$ .

In Figure 4 we show the energy width from EDC curves as a function of binding energy  $\tilde{\omega}(\mathbf{k})$ . The data show a discontinuity in the width of the quasiparticle peak at the same energy corresponding to the kink in  $\tilde{\omega}(\mathbf{k})$ . Besides, since EDC width is interpretable as the inverse

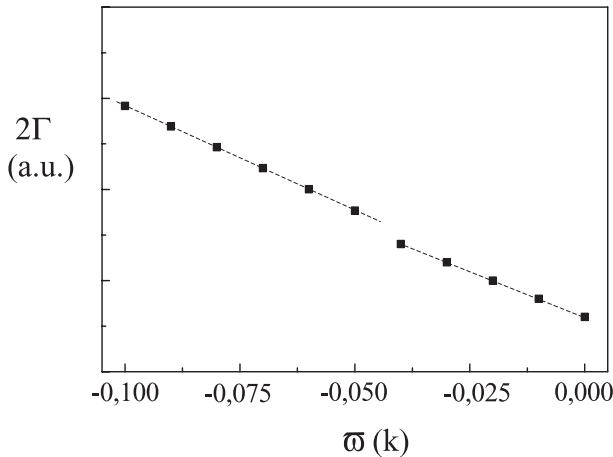


**Fig. 4.** Full width of the EDC curves in arbitrary units (a.u.) as a function of the maximum position  $\tilde{\omega}(\mathbf{k})$  (binding energy). The dashed line represents a linear fit of the high and low energy parts of the width. We observe a drop in the linear slope around  $-0.05$  eV corresponding to the energy of the kink.

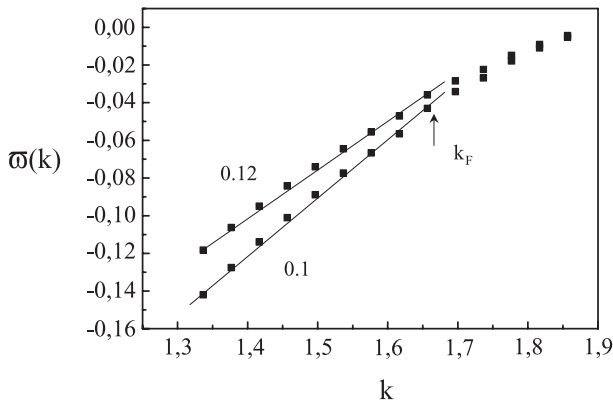


**Fig. 5.** Quasiparticle dispersion along the nodal Brillouin line for two values of the doping  $\delta = 0.12, 0.1$ . The straight lines represent the linear fit of the low-energy part. As shown in the figure the quasiparticle velocity (i.e. the linear slope) decreases with doping.

quasiparticle lifetime  $1/\tau$ , the results immediately show a non-Fermi-liquid behavior associated with a linear dependence of the width below and above the kink energy (dashed line). Other results have been finally obtained at varying doping. In Figure 5 we report the quasiparticle spectrum for the values of the doping  $\delta = 0.12, 0.1$ . When we decrease the doping, the kink feature slightly moves to lower binding energies (from  $-0.04$  meV to  $-0.05$  meV) showing that the energy scale of the kink is related to the doping. The results in Figure 5 also show that the quasiparticle velocity (i.e. the linear coefficient) decreases with doping, in agreement with recent high-resolution photoemission experiments [20] on Bi2212.

Concluding, by using a strong coupling approach based on a cumulant expansion in an extended two dimensional Hubbard model, we have shown that the anomalous

quasiparticle features experimentally observed in the normal state of  $\text{Bi}_2\text{Sr}_2\text{CaCu}_2\text{O}_{8+\delta}$  (Bi2212) can be well described in terms of the coupling of the charge carriers to an incommensurate charge density wave (ICDW) with a critical vector oriented along the diagonal direction. Our results show that low-energy charge mode contribute to the formation of a kink in the quasiparticle spectrum along the nodal direction at energies around 50 meV, in agreement with ARPES experiments in Bi2212. We have also shown that the presence of critical charge fluctuations manifests in a linear behavior on the quasiparticle inverse lifetime as a function of the binding energy, with a drop in the slope at the energy of the kink. The analysis of the spectrum at varying doping shows that the quasiparticle velocity decreases with  $\delta$  in agreement with recent photoemission experiments. We would like to stress that the last feature is the most difficult to interpret in the other scenarios proposed for the kink and put a stone in favor of the stripe scenario. It would be interesting to extend the present analysis to the presence of superconducting quasiparticles and to include the effect of fluctuating stripes in order to describe recent experiments on LSCO systems.

We would like to acknowledge Prof. K. Nakagawa and Prof. M. Grilli for helpful discussions.

## References

1. S. Massidda et al., *Physica C* **152**, 251 (1988); H. Krakauer, W.E. Pickett, *Phys. Rev. Lett.* **60**, 1665 (1988)
2. A. Kaminski et al., *Phys. Rev. Lett.* **84**, 1788 (2000)
3. P.V. Bogdanov et al., *Phys. Rev. Lett.* **85**, 2581 (2000)
4. A. Lanzara et al., *Nature* **412**, 510 (2001); Z.-X. Shen, A. Lanzara, S. Ishihara, N. Nagaosa, *Phil. Mag. B* **82**, 1349 (2002)
5. J.C. Campuzano et al., *Phys. Rev. Lett.* **83**, 3709 (1999)
6. M. Eschrig, M.R. Norman, *Phys. Rev. Lett.* **85**, 3261 (2000)
7. A. Kaminski et al., *Phys. Rev. Lett.* **86**, 1070 (2001)
8. G. Seibold, M. Grilli, *Phys. Rev. B* **63**, 224505 (2001)
9. R. Citro, M. Marinaro, *Eur. Phys. J. B* **20**, 343 (2001)
10. C. Castellani, C. Di Castro, M. Grilli, *Phys. Rev. Lett.* **75**, 4650 (1995); C. Castellani, C. Di Castro, M. Grilli, *Z. Phys. B* **103**, 137 (1997)
11. C. Bernhard et al., *Phys. Rev. Lett.* **86**, 1614 (2001) and references therein
12. C. Howald, H. Eisaki, N. Kaneko, M. Greven, A. Kapitulnik, *Phys. Rev. B* **67**, 14533 (2003)
13. V.A. Moskalenko, L.Z. Kon, *Cond. Matt. Phys.* **1**, 23 (1998)
14. W. Metzner, *Phys. Rev. B* **43**, 8549 (1991)
15. R. Citro, M. Marinaro, *Int. J. Mod. Phys.* **14**, 3000 (2000)
16. S. Caprara, M. Sulpizi, A. Bianconi, C. Di Castro, M. Grilli, *Phys. Rev. B* **59**, 14980 (1999)
17. N.L. Saini et al., *Phys. Rev. Lett.* **79**, 3467 (1997)
18. T. Valla et al., *Phys. Rev. Lett.* **83**, 2085 (1999)
19. R. Citro, M. Marinaro, *Eur. Phys. J. B* **28**, 55 (2002)
20. P.D. Johnson et al., *Phys. Rev. Lett.* **87**, 177007 (2001)